A Non-Invasive, Machine Learning Assisted Skin-Hydration Microwave Sensor

A Non-Invasive, Machine Learning Assisted Skin-Hydration Microwave Sensor

S. Trovarello[1], O. Afif[2], A. Di Florio Di Renzo[3], D. Masotti[4], M. Tartagni[5], and A. Costanzo[6]

DEI-"Guglielmo Marconi", University of Bologna, Italy

{[1]simone.trovarello2, [2]oumaima.afif2, [3]alessandra.diflorio3, [4]diego.masotti, [5]marco.tartagni, [6]alessandra.costanzo}@unibo.it

Abstract — This paper presents a non-invasive and electrode-less skin-hydration sensor based on a microwave resonator, assisted by a machine learning (ML) classification algorithm. A miniaturized complementary-split ring resonator (CSRR) operating in the 2÷3 GHz band is designed to sense and detect hydration changes in the human skin utilizing the near-field interaction with the resonator. The resonator is first simulated using electromagnetic (EM) simulations and loaded with skin in different hydration conditions. Then, the resonator is fabricated and tested in three different body regions: thenar eminence, proximal wrist ceases, and cheek. Spectra are collected during an extensive experimental campaign in which repeated measurements are taken over three days on the three regions of the body. The Soft Independent Modelling of Class Analogy (SIMCA) method is then used to interpret and classify the spectral data acquired from the resonator into two distinct hydration classes. The results of this study highlight the effectiveness of SIMCA as a multivariate analysis technique for processing and categorizing spectral data obtained from CSRR for monitoring body hydration. This approach provides a cost-effective solution and demonstrates high efficiency in accurately distinguishing between hydration states, which holds great promise for practical applications in hydration monitoring.

Keywords — CSRR, microwave sensor, skin hydration, multivariate analysis.

I. Introduction

There is increasing interest in applying microwave sensors across diverse biomedical fields. Significant advantages of these sensors include their noninvasive nature and utilization of non-ionizing radiation. Additionally, they offer rapid measurements and are cost-effective to manufacture. Most of the solutions are resonance-based sensors, exploiting split-ring resonators (SRRs), complementary split-ring resonators (CSRRs), and planar antennas [1-3]. At the same time, machine learning has increased rapidly in recent years. This can be primarily attributed to two key factors: the increased accessibility of computing power and the widespread digitization of data, facilitated by sensors across a multitude of applications, such as dielectric characterization, temperature variation detection, breast cancer detection, and measurement of glucose in blood [4-7].

Maintaining proper water levels is crucial for human health, as deviations from this balance can impair cognitive and physical abilities. For instance, variations in the levels of water concentration in the epidermis are associated with various skin disorders, including burns, edema, inflammation, and skin cancer. In the literature, several technologies are adopted to measure the hydration status of the skin [8-10]. However, these techniques are expensive and not widely available. Additionally, they require large devices that are not portable, making them impractical for use in screening procedures. Furthermore, some of these methods do not incorporate machine learning algorithms, which could further enhance the system's accuracy. This reliance on extensive data processing underscores the complex nature of hydration assessment. The studies conducted in [11] emphasize the necessity for robust management of data acquisition and advocate for a greater focus on developing more portable and flexible hardware solutions.

This paper presents a resonator-based skin hydration sensor employing a low-cost CSRR in the 2.4 GHz band, with a topology like the one presented in [12]. This work proposes a different operating frequency and includes the integration with ML models. Furthermore, this demonstrates the integration of the results of a classification model algorithm and a low-cost, non-invasive, portable, and wearable microwave sensor probe consisting of a CSRR. The algorithm is based on a small dataset and statistical analysis to predict the hydration status of the human body directly from skin-sensing measurements.

II. Sensor Design and Fabrication

The microwave sensor is based on a CSRR in the 2.4 GHz ISM band. The working principle is based on the near-field interaction between the fringing effect of the electric field and the skin under different hydration conditions. The EM field lines are modified by the interaction with the skin under test, thus affecting the resonance frequency of the loaded CSRR (the equivalent capacitance of the LC circuit is modified accordingly).

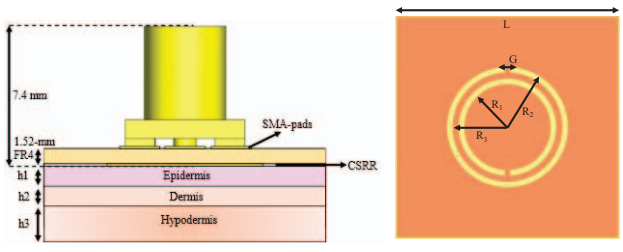

(a) (b)

Fig. 1. Lateral (a), and bottom (b) view of the proposed CSRR-based skin hydration sensor. h1, h2, and h3 are set to 1 mm, 1 mm, and 4 mm respectively.

Concerning the traditional split-resonator topology, the complementary alternative can be seamlessly fabricated onto an SMA connector. With its large ground area, the external part of

the resonator can be easily connected to the outer nut of the RF connector. In contrast, the hot wire is directly connected to the inner part of the resonator.

The resonator is designed on a low-cost FR4 PCB (ε_r=4.3, tanδ=0.025). Five via holes are placed in the five pins positions of the SMA connector, to shorten the top and bottom part of the 1.52-mm thick PCB. This configuration guarantees high mechanical robustness and an easy fabrication process of the resonator. Figs. 1 show the lateral (a) and bottom (b) view of the designed resonator, where the geometrical dimensions of the resonator are reported (G= 0.2 mm, R_1=1.5 mm, R_2=2.1 mm, R_3=1.9 mm, and L=8 mm). An 8-µm PTE layer is placed below the sensor to avoid direct contact between the metal layer and the skin, making the sensor electrode-less. Three layers (epidermis, dermis, and hypodermis) are used to electromagnetically represent the human skin. Typical thickness and electrical properties of the skin layers, reported in [12]-[13], are used. The CSRR-based sensor is designed using full-wave simulations in CST STUDIO SUITE.

The skin penetration depth is first predicted by EM simulation in terms of the E-field density in the presence of the CSRR. For comparison, the same computation has been carried out for a patch antenna at the same operating frequency. The corresponding results are superimposed in Fig. 2.

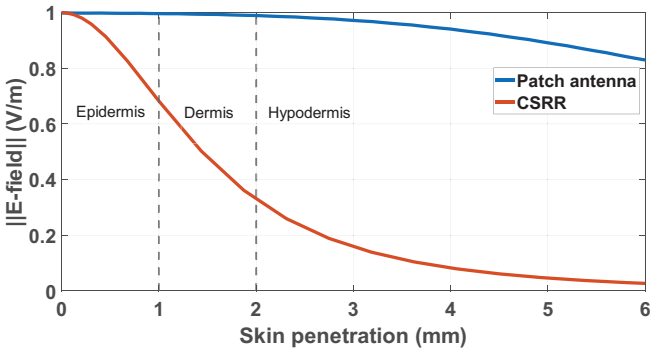

Fig. 2. Normalized electric-field decay inside the multi-layer skin simulated phantom from starting from the PTE-coated CSRR (0 mm) and the limit of the upper limit of the phantom (6 mm), in case of a patch antenna and a CSRR operating in the same frequency band.

As expected, the penetration depth of the electric field obtained by loading the patch antenna with the skin is significantly greater than in the case of CSRR. It can be noted that with the patch antenna, after 6 mm, the electric field's strength only decreases by 20%, allowing it to pass through the biological tissues beneath the skin. This results in a reduction in the resonator's sensing capabilities since most of the water content resides in the most superficial area of the skin. Consequently, a patch antenna, and in general a resonator operating in the near-field radiative region, is not suitable for skin sensing applications. While, the CSRR loaded with the skin shows a decrease in electric field intensity of 32% and 65% at 1- and 2-mm depth, respectively. This allows to confirm the choice of a CSRR, operating in the non-radiative near-field region.

Fig. 3 shows the simulated behaviors of the reflection coefficients calculated at the SMA port of the loaded CSRR. EM simulations demonstrate that variations in skin permittivity highly influence the resonator's sensitivity, and consequently, the hydration state variations. For the normal skin a return loss of 17.6 dB is observed at 2060 MHz, while for the hydrated and dehydrated, the peaks are shifted to 2024 MHz and 2116 MHz, respectively.

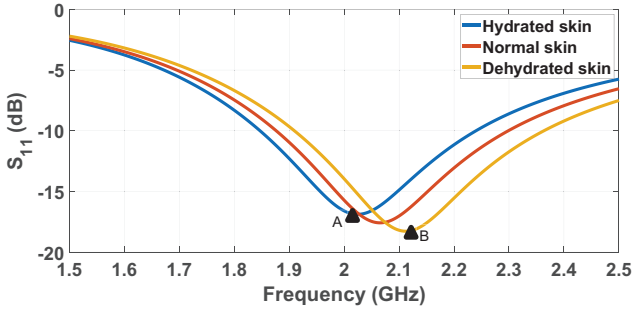

Fig. 3. EM-simulated behavior of the reflection coefficient calculated at the SMA connector input port. A 92-MHz frequency shift, calculated as B-A, is observed between the lowest and highest level of hydration simulated.

III. Validation Measurements and Machine-Learning Integration

A. Data Acquisition Procedures and Multivariate Modeling

Figs. 4 show the top and bottom view of the fabricated CSRR on the FR4 substrate. The total dimensions of the prototype are 1.4 cm x 1.4 cm x 0.74 cm.

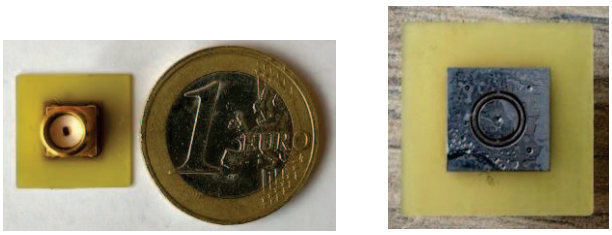

(a) (b)

Figs. 4. Top-view (a), and bottom-view (b) of the fabricated resonator for skin hydration sensing purposes.

Systematic spectral acquisitions over different human anatomical areas are performed twice daily. Measurements were taken with custom hardware containing a low-cost VNA, governed by a Raspberry Pi connected to the CSRR, which facilitated measurements at any location on the body.

The volunteer performs a 12-hour fasting (of both solid and liquid food and drink) during the day, where the first set of measurements is carried out after 6 hours from the beginning of the fast (t_1). The second measurement is carried out after 14 hours from the beginning (t_2). This leads to an approximately 8-hour interval between the two sets of measurements. The proposed experimental campaign has been repeated for two days.

The study is focused on examining hydration levels in the thenar eminence, in the proximal wrist crease of one hand, and on the cheek. This selection of anatomical sites ensures a

focused investigation of hydration dynamics. For each anatomical site selected, a total of 2 x N (where $N > 3$) is acquired. Each acquisition lasts approximately 1 minute, ensuring a thorough and detailed examination of the spectral data for comprehensive analysis.

A classification model, differentiating between hydration conditions based on amplitude variations of the measured reflection coefficient is developed. The model is derived through the application of Soft Independent Modelling of Class Analogy (SIMCA), based on multivariate statistical analysis [14]-[15]. The process is divided into three steps: model creation, cross-validation, and validation, as shown in Fig 5. The calibration sets are created using measurements taken on the selected area on the volunteer body.

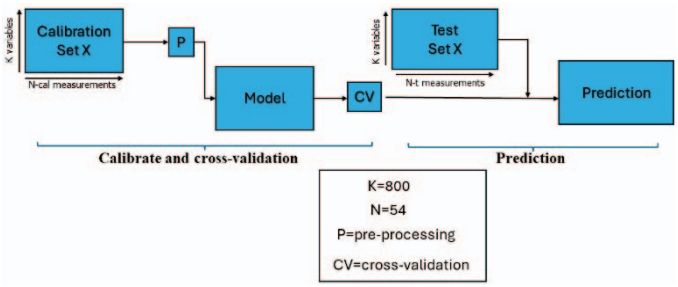

Fig. 5. Representation of the workflow used in the SIMCA algorithm.

Then, the independent variables are arranged in K=800 (variables, spectrum points) times N=54 (measurements) matrix ($\boldsymbol{X}$ dataset). The complete dataset is used to create the training and test sets, with 80% allocated for calibration and 20% for testing, chosen randomly and equally distributed between all the classes. The model assigns these spectra to different classes, and the results are compared to the actual class. This comparison produces a confusion matrix, where rows describe the actual class of the measured result, while columns are the predicted classification, together with characterization parameters. These outputs describe the robustness of the SIMCA model, as we will discuss in the next section.

B. Measurements and Multivariate Modeling Results

The measurement setup and the acquired spectra are illustrated in Figs. 6. Measurements demonstrate a visible frequency shift in all three analyzed body regions. An increase in the resonant frequency of the resonator is visible from t_1 and t_2 measurements. For the thenar eminence, a 75 MHz shift can be observed, while for the proximal wrist ceases and the cheek the observed shifts are 90 and 143 MHz, respectively. This observed trend provides a promising basis for constructing statistical models.

Measurements confirm the predicted hydration-related reflection coefficients simulated in Fig. 3. It is reasonable to infer that the measured spectra at time t_2 exhibit a higher resonant frequency, as instance t_1 occurs shortly after the start of fasting and still reflects the impact of food and liquids consumed. Henceforth, can be concluded that the instant t_1 represents the hydrated condition of the skin, while the instant t_2 represents the dehydrated state.

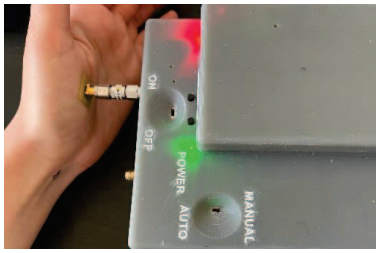

(a)

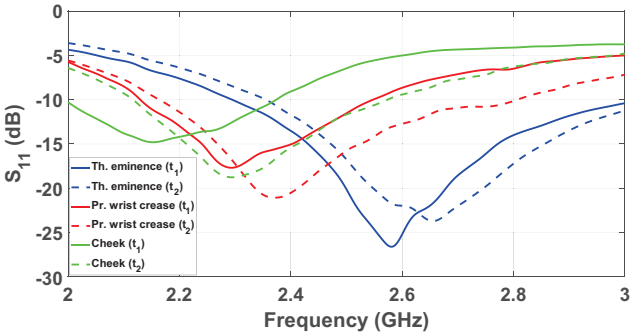

(b)

Figs. 6. (a) Measurement setup and, (b) the measured average of N acquired spectra for each position, in t_1 and t_2.

However, spectra can be influenced by the noise stemming from both machine and human errors. As a result, the spectra underwent preprocessing to eliminate outliers before being utilized as the inputs of the SIMCA analysis, auto-scale, and the Savitsky-Golay preprocessing were applied to the $\boldsymbol{X}$ dataset. This involved centering and scaling each variable to unit standard deviation. The spectra underwent a polynomial transformation and cross-terms to address its non-linear trend. Two errors for both cross-validation and calibration can be defined: Root Mean Square Error of Cross-Validation (RMSECV) and Root Mean Square Error of Calibration (RMSEC). For t_1, the RMSECV and RMSEC are 0.3908 and 0.2397 respectively, while for t_2 condition, the RMSECV is 0.4359, and the RMSEC is 0.2511. Table 1 shows the confusion matrix, which provides a comprehensive overview of the model's performance in predicting hydration levels at two distinct time points, t_1 and t_2. It allows for a detailed comparison between predicted and actual values, highlighting areas of accuracy and discrepancy. In particular, the matrix highlights that the values on the diagonal should be maximized for precise identification of skin hydration class, indicating accurate predictions. At t_1, all 27 instances were accurately predicted, indicating perfect model performance for this time point. Similarly, at t_2, 24 instances were accurately predicted, showing high accuracy. Off-diagonal values indicate misclassifications. At t_1, no instances were misclassified, reinforcing the model's perfect accuracy for this time point. However, at t_2, 3 instances were incorrectly predicted as t_1, highlighting an area where the model's performance can be improved by providing more measurements.

The model's overall performance highlights satisfactory results even when dealing with small datasets (N=54), with minimal misclassification. Moreover, Table 2 shows the statistical parameters, both obtained from the SIMCA model.

Table 1. Confusion matrix.

	Predicted hydrated in t_1	**Predicted hydrated in t_2**
Actual hydration in t_1	27	0
Actual hydration in t_2	3	24
Unsigned class	0	0

Table 2. Statistical parameters were calculated from the confusion matrix.

Class	**Err**	**F1**
Hydration in t_1	0.25926	0.80412
Hydration in t_2	0.25926	0.75000

The most promising outcome lies in the low misclassification error (Err) and the high F1 score, defined as the harmonic means of both sensitivity and precision, achieved for each class. This indicates a strong classification performance, highlighting both accuracy and balance between precision and sensitivity for the two classes, despite the small dataset. Once the predictive model is set up offline, it can smoothly integrate into embedded and/or autonomous devices alongside CSRR, VNA, and other components, thanks to their low computational needs. Overall, this machine learning model streamlines data processing by extracting relevant features and reducing dimensionality by identifying trends and relationships within the data. At the same time, its ability to recognize patterns, detect anomalies, and provide decision support for interpretation leads to more informed decision-making.

IV. Conclusion

This paper presents a non-invasive and cost-effective microwave skin hydration sensor based on a CSRR-resonator, integrated with a classification model able to distinguish hydration classes in different human body regions. The CSRR is designed to operate in the 2÷3 GHz band and is fabricated and tested with a two-day measurements campaign, where several spectra are acquired on thenar eminence, proximal wrist ceases, and cheek. Measurements are then post-processed with an ML model based on statistical analysis, using the SIMCA algorithm. The low misclassification error and high F1 score demonstrate the ability of the model and the sensor, in general, to distinguish hydration levels in human skin with small input datasets. This approach holds promise for creating autonomous, non-invasive devices for real-time hydration monitoring. Moreover, this method can be adjusted and therefore implemented to any electrical quantity that shows any hydration-related variations in skin, broadening its application across various fields.

Acknowledgment

We want to acknowledge Leonardo Franceschelli for the electronic setup and design and Giovanni Innocenti, M.D., for inspiration for the device and suggestions on in vivo tests.

References

[1] P. Vélez, L. Su, K. Grenier, J. Mata-Contreras, D. Dubuc and F. Martín, "Microwave Microfluidic Sensor Based on a Microstrip Splitter/Combiner Configuration and Split Ring Resonators (SRRs) for Dielectric Characterization of Liquids," in IEEE Sensors Journal, vol.17, no. 20, pp. 6589-6598, 15 Oct.15, 2017.

[2] L. Su, J. Mata-Contreras, P. Vélez and F. Martín, "Splitter/Combiner Microstrip Sections Loaded With Pairs of Complementary Split Ring Resonators (CSRRs): Modeling and Optimization for Differential Sensing Applications," in IEEE Transactions on Microwave Theory and Techniques, vol. 64, no. 12, pp. 4362-4370, Dec. 2016.

[3] A. Di Florio Di Renzo, S. Trovarello, O. Afif, L. Franceschelli, M. Tartagni, D. Masotti, A. Costanzo, "A Stand-Alone Moisture Content Sensor Based on a Loaded Self-Oscillating Antenna," 2024 IEEE/MTT-S International Microwave Symposium - IMS 2024, Washington, DC, USA, 2024.

[4] C. Gocen and M. Palandoken, "Machine Learning Assisted Novel Microwave Sensor Design for Dielectric Parameter Characterization of Water–Ethanol Mixture," in IEEE Sensors Journal, vol. 22, no. 3, pp. 2119-2127, 1 Feb.1, 2022.

[5] N. Kazemi, M. Abdolrazzaghi and P. Musilek, "Comparative Analysis of Machine Learning Techniques for Temperature Compensation in Microwave Sensors," in IEEE Transactions on Microwave Theory and Techniques, vol. 69, no. 9, pp. 4223-4236, Sept. 2021.

[6] T. Reimer and S. Pistorius, "The Diagnostic Performance of Machine Learning in Breast Microwave Sensing on an Experimental Dataset," in IEEE Journal of Electromagnetics, RF and Microwaves in Medicine and Biology, vol. 6, no. 1, pp. 139-145, March 2022.

[7] A. E. Omer, G. Shaker and S. Safavi-Naeini, "Portable Radar-Driven Microwave Sensor for Intermittent Glucose Levels Monitoring," in IEEE Sensors Letters, vol. 4, no. 5, pp. 1-4, May 2020.

[8] L. Peng et al., "A Fused Learning and Enhancing Method for Accurate and Noninvasive Hydration Status Monitoring With UWB Microwave Based on Phantom," in IEEE Transactions on Microwave Theory and Techniques, vol. 71, no. 9, pp. 4027-4036, Sept. 2023.

[9] A. Cataldo et al., "Portable Microwave Reflectometry System for Skin Sensing," in IEEE Transactions on Instrumentation and Measurement, vol. 71, pp. 1-8, 2022.

[10] S. Bing, K. Chawang and J.-C. Chiao, "A Flexible Tuned Radio-Frequency Planar Resonant Loop for Noninvasive Hydration Sensing," in IEEE Journal of Microwaves, vol. 3, no. 1, pp. 181-192, Jan. 2023.

[11] A. Cataldo, E. De Benedetto, R. Schiavoni, G. Monti, A. Tedesco, A. Masciullo, E. Piuzzi, and L. Tarricone, "Portable microwave reflectometry system for skin sensing," IEEE Transactions on Instrumentation and Measurement, vol. 71, pp. 1–8, 2022.

[12] J. Kilpijärvi, J. Tolvanen, J. Juuti, N. Halonen and J. Hannu, "A Non-Invasive Method for Hydration Status Measurement With a Microwave Sensor Using Skin Phantoms," in IEEE Sensors Journal, vol. 20, no. 2, pp. 1095-1104, 15 Jan.15, 2020.

[13] Hasgall PA, Di Gennaro F, Baumgartner C, Neufeld E, Lloyd B, Gosselin MC, Payne D, Klingenböck A, Kuster N, "IT'IS Database for thermal and electromagnetic parameters of biological tissues," Version 4.1, Feb 22, 2022.

[14] S. Wold, K. Esbensen, and P. Geladi, "Principal component analysis," Chemometrics and intelligent laboratory systems, vol. 2, no. 1-3, pp. 37–52, 1987.

[15] L. Franceschelli et al., "Non-intrusive microwave technique for direct detection of concrete compressive strength monitoring by multivariate modeling," Measurement, vol. 206, p. 112332, Jan. 2023.